doi: 10.32023/0001-5237/72.3.1

ACTA ASTRONOMICA
Vol. **72** (2022) pp. 161–170

New Short-Period δ Scuti Stars in OGLE-IV Fields toward the Galactic Bulge*

P. Pietrukowicz[1], M. Ratajczak[1], I. Soszyński[1], A. Udalski[1], M.K. Szymański[1], K. Ulaczyk[2], R. Poleski[1], S. Kozłowski[1], J. Skowron[1], D.M. Skowron[1], P. Mróz[1], K. Rybicki[1,3], P. Iwanek[1], M. Wrona[1] and M. Gromadzki[1]

[1] Astronomical Observatory, University of Warsaw, Al. Ujazdowskie 4, 00-478 Warszawa, Poland
[2] Department of Physics, University of Warwick, Coventry CV4 7AL, UK
[3] Department of Particle Physics and Astrophysics, Weizmann Institute of Science, Rehovot 76100, Israel

Received November 7, 2022

ABSTRACT

We report the classification of 24 puzzling short-period variable stars located in OGLE-IV Galactic bulge fields. The stars are low-amplitude (< 0.05 mag) multi-periodic objects with dominant periods between 22 min and 54 min whose type could not have been unambiguously established based on photometry only. A low-resolution spectroscopic follow-up observations have shown that all the objects are main sequence A/F-type stars. Thus, all the variables are δ Sct-type pulsators. We have added them to the OGLE-IV Collection of Variable Stars.

Key words: *Catalogs – Stars: variables: delta Scuti – Galaxy: bulge – Galaxy: disk*

1. Introduction

δ Sct-type variable stars are pulsating stars with periods below 0.3 d and *V*-band (*I*-band) amplitudes up to 0.9 mag (0.6 mag). Most of them are multiple-mode pulsators (Netzel *et al.* 2022). They have spectral types from A0 to F6 and luminosity classes from III (giants), through IV (subgiants), to V (dwarfs). In the Hertzsprung–Russell diagram, δ Sct stars reside in the part where the classical instability strip intersects the main sequence (MS). They can also be found in the

*Based on photometric observations obtained with the 1.3-m Warsaw telescope at Las Campanas Observatory of the Carnegie Institution for Science and spectroscopic data collected with the European Southern Observatory (ESO) NTT telescope at La Silla Observatory under ESO programme 105.20EF.001.

pre-MS and post-MS stages. Space-based observations from the Kepler satellite revealed that no more than 70 per cent of all stars in that part pulsate (Murphy *et al.* 2019). The Kepler data also showed that the majority of δ Sct stars are low-amplitude pulsators (< 0.1 mag) and only about half of them have amplitudes > 0.001 mag and appear to be variable in ground-based observations (Balona and Dziembowski 2011).

The upper bound of 0.3 d (7.2 h) for fundamental-mode δ Sct stars was arbitrarily set due to scarcity of Population I classical pulsators with periods in the range of 0.3–1 d. Stars with periods longer than 0.3 d are classified as classical Cepheids (Soszyński *et al.* 2008). Until the early 2010s, shortest periods of the known δ Sct-type stars were of about 25–30 min (*e.g.*, 25.54 min in ω Cen V294, 26.25 min in ω Cen V295 – Kaluzny *et al.* 2004). Holdsworth *et al.* (2014) searched for high-frequency signals in SuperWASP data and reported on the detection of over 350 candidates for short-period pulsators including δ Sct stars with periods in the range of 6–29 min.

Classification of variable stars with periods below 1 h (≈ 0.042 d) purely based on photometry is often very difficult due to low amplitudes and sinusoidal shapes of the light curves. A position in the color–magnitude diagram is usually insufficient to indicate the true variability type, particularly in the case of heavily reddened objects located close to the Galactic plane. There are many types of pulsating stars with periods below 1 h. Among them there are various types of white dwarfs (*e.g.*, ZZ Cet, V777 Her – Winget and Kepler 2008), pre-white dwarfs (*e.g.*, EL CVn – Maxted *et al.* 2013), hot subdwarfs (*e.g.*, V361 Hya, V1093 Her – Heber *et al.* 2016), Blue Large-Amplitude Pulsators (Pietrukowicz *et al.* 2017, Kupfer *et al.* 2019), objects from the GW Vir family including planetary nebulae nuclei variables (PNNV, Quirion *et al.* 2007), δ Sct stars (Rodríguez *et al.* 2000), and their Population II analogues, SX Phe stars (Rodríguez and López-González 2000). There is also a group of rapidly oscillating Ap (roAp) variables showing light variations in the range of 4.7–25.8 min and amplitudes of millimagnitudes or smaller (Kurtz 2022). Recent analysis of TESS observations indicates that these variables should be treated as normal δ Sct stars and the term "roAp" should be avoided (Balona 2022). Definitive classification of short-period variables often requires a spectroscopic confirmation. This is the case of objects presented in the work here.

Searches for short-period variables in 121 OGLE-IV fields covering the inner Galactic bulge and central part of the Sagittarius Dwarf Spheroidal Galaxy brought the identification of a total of 10 140 δ Sct stars with periods in the range of 0.033–0.3 d (47.7 min–7.2 h) (Pietrukowicz *et al.* 2020, Soszyński *et al.* 2021). The main criteria used in the classification process were the period value and asymmetry in the light curve shape. In addition to this set, 157 extremely short variables with periods in the range of 0.01–0.04 d (14.4–57.6 min) were found but could not have been unambiguously classified. From this sample, 24 stars with sinusoidal variations stable over years and located in the upper part of the MS in the color–

magnitude diagrams were subject of our spectroscopic follow-up. In Section 2 we provide details on the photometric and spectroscopic observations. Information on the 24 targets selected for the spectroscopic campaign can be found in Section 3, while the results are presented in Section 4.

2. Observations

Photometric observations were obtained in the framework of a long-term variability survey, the Optical Gravitational Lensing Experiment (OGLE), conducted on the 1.3-m Warsaw telescope at Las Campanas Observatory, Chile. The analyzed in this work data were collected during the fourth phase of the survey (OGLE-IV) in years 2010–2019. OGLE monitors the Milky Way's bulge and disk and Magellanic Clouds in searches for periodic and irregular brightness variations as well as for transient events. The entire monitored area covers about 3600 $\deg^2$. The OGLE-IV camera is a mosaic of 32 CCD detectors covering a field of 1.4 $\deg^2$ at a scale of 0.26 arcsec/pixel. Most of the observations were taken through the Cousins *I* filter. The remaining data were taken through the Johnson *V* filter to secure color information. Over the whole decade in the area of the inner Galactic bulge, OGLE collected about 181 500 *I*-band frames and 6400 *V*-band frames. The number of *I*-band measurements per object varies from 60 up to 16 800, depending on the field. The exposure times were of 100 s in *I* and 150 s in *V*. In the case of three most crowded fields, BLG501, BLG505, and BLG512, the cadence of *I*-band observations was as short as 19 min. Time-series photometry was extracted using the Difference Image Analysis (DIA – Woźniak 2000), a technique developed especially for dense stellar fields (Alard and Lupton 1998). Observations of the inner bulge cover a magnitude range of $12.5 < I < 21.5$. Technical details on the OGLE survey can be found in Udalski *et al.* (2015). The OGLE-IV Collection of Variable Stars (OCVS) contains over one million objects of various variability types: pulsating stars (*e.g.,* Soszyński *et al.* 2019), spotted stars (*e.g.,* Iwanek *et al.* 2019), eclipsing and ellipsoidal binaries (*e.g.,* Pawlak *et al.* 2016, Wrona *et al.* 2022), cataclysmic systems (*e.g.,* Mróz *et al.* 2015). Despite the huge number of known variable stars, some of newly detected objects are puzzling and require spectroscopic investigation to properly classify them and to understand their nature.

Low-resolution spectroscopic observations were conducted under ESO programme 105.20EF.001 in remote visitor mode (due to Covid-19 pandemic restrictions) over four consecutive nights in gray time, from 2021 June 30/July 1 to July 3/4. The spectra were collected with the ESO Faint Object Spectrograph and Camera 2 (EFOSC2) mounted at the Nasmyth focus of the 3.58-m New Technology Telescope (NTT) located at La Silla Observatory, Chile. Information about the characteristics of this instrument are provided in Buzzoni *et al.* (1984). Thin cirrus clouds were present during the whole observing run but the first half of the third night when they were thick. All the spectra were taken with grism #4 covering wavelengths 4085–7520 Å at the slit width of $1\farcs0$ and 2×2 binning read-

out, which provided a spectral resolution of about 11 Å at 5000 Å. For most of the objects the slit was aligned to the parallactic angle, but in some cases the slit was oriented properly to avoid light from neighboring stars. Exposure times were calculated with the help of the ESO Exposure Time Calculator[†] to obtain spectra with a signal-to-noise ratio of 50. For wavelength calibrations, the He-Ar lamp was used. Three spectrophotometric standard stars were selected for the flux calibrations. Bias and dome flat-field images were taken at dawn. All spectra were reduced using the IRAF package[‡]. Debiasing, flat-fielding, wavelength and flux calibrations were performed in the standard way.

3. Target Objects for the Spectroscopic Follow-up

In Table 1, we provide information on the 24 stars selected for our spectroscopic run. The stars are located toward the Galactic bulge. They have magnitudes in the range of $13.1 < I < 15.6$ and $14.2 < V < 17.5$. All the stars are multi-periodic variables with amplitudes below 0.05 mag in *I*. We list up to five detected periodicities. The periods were determined with the help of the TATRY code (Schwarzenberg-Czerny 1996) after subsequent pre-whitenings.

4. Results from the Spectroscopic Observations

In Figs. 1–2, for each star, we present the OGLE-IV *I*-band light curve folded with the dominant period, a color–magnitude diagram with the position of the star, and the obtained EFOSC2 spectrum. The spectra of all stars are dominated by the Balmer series, which indicates type A. In all the stars, one can also spot the blended sodium doublet NaI (D1: 5896 Å, D2: 5890 Å), which is primarily of interstellar origin for this spectral type.

A detailed analysis of the spectra was carried out with the iSpec package (Blanco-Cuaresma *et al.* 2014, Blanco-Cuaresma 2019). To determine atmospheric parameters, the effective temperature $T_{\rm eff}$ and surface gravity $\log g$, we used the MARCS model atmosphere (Castelli and Kurucz 2003), Synthe radiative code (Kurucz 2005), solar abundances provided in Asplund *et al.* (2009), and VALD atomic line list (Piskunov *et al.* 1995). Due to the low spectral resolution, our analysis was based on the Balmer lines only (Hα, Hβ, and Hγ). The parameters $T_{\rm eff}$ and $\log g$ were fitted with starting values of 7000 K and 4.0, respectively. Microturbulence velocity was fixed at 2 km/s, while macroturbulence velocity at 4 km/s. The rotational velocity $v \sin i$ was assumed to be of 5 km/s and the metallicity [M/H] of 0.0 dex. Results of the analysis are collected in Table 2. In Fig. 3, we present normalized spectra for three shortest-period δ Sct stars in our sample with models obtained from the spectral synthesis.

[†] *https://www.eso.org/observing/etc/*

[‡] IRAF was distributed by the National Optical Astronomy Observatory, USA, which is operated by the Association of Universities for Research in Astronomy, Inc., under a cooperative agreement with the National Science Foundation.

Table 1

Photometric parameters of the 24 target stars

Name OGLE-BLG-DSCT-	RA(2000)	Dec(2000)	$\langle I \rangle$ [mag]	$\langle V \rangle$ [mag]	P_1 [d]	P_2 [d]	P_3 [d]	P_4 [d]	P_5 [d]
16860	$17^h22^m51\overset{s}{.}74$	$-30°16'23\overset{''}{.}1$	15.53	17.49	0.033531956(24)	0.036224500(35)	0.042320454(45)	–	–
16861	$17^h32^m20\overset{s}{.}04$	$-22°05'49\overset{''}{.}1$	13.10	14.20	0.034233043(20)	0.039879897(52)	0.016609671(15)	–	–
16862	$17^h35^m57\overset{s}{.}82$	$-26°54'50\overset{''}{.}6$	14.34	15.72	0.035165296(11)	0.038645168(18)	0.040651018(27)	0.045402275(52)	0.035165937(64)
16863	$17^h38^m33\overset{s}{.}75$	$-34°09'26\overset{''}{.}4$	14.85	16.65	0.035719287(23)	0.039362439(60)	0.08913910(39)	0.043655649(97)	0.04184227(10)
16864	$17^h44^m34\overset{s}{.}25$	$-33°17'56\overset{''}{.}1$	15.28	16.76	0.035541111(20)	0.09749517(25)	0.051245588(88)	–	–
16865	$17^h47^m50\overset{s}{.}67$	$-20°48'46\overset{''}{.}4$	15.17	16.53	0.037076495(22)	0.046284106(35)	0.04357615(11)	–	–
16866	$17^h50^m02\overset{s}{.}34$	$-33°18'59\overset{''}{.}5$	14.48	15.71	0.033961025(13)	0.037164189(44)	0.036201125(56)	–	–
16867	$17^h50^m31\overset{s}{.}18$	$-29°28'06\overset{''}{.}3$	15.06	16.30	0.025409872(10)	0.027650646(25)	0.029687043(47)	0.032681617(62)	0.029680207(58)
16868	$17^h51^m35\overset{s}{.}11$	$-28°44'39\overset{''}{.}2$	15.11	16.10	0.0278339039(50)	0.032812117(21)	0.06660964(12)	0.027834329(29)	0.047779888(96)
16869	$17^h51^m46\overset{s}{.}46$	$-28°26'05\overset{''}{.}3$	15.08	15.93	0.0190090983(40)	0.0201545952(54)	0.0201278558(72)	0.0201484003(80)	0.0213994311(96)
16870	$17^h51^m55\overset{s}{.}89$	$-30°17'18\overset{''}{.}9$	14.66	15.79	0.0255401151(79)	0.027133418(24)	0.027149755(35)	0.028792153(40)	–
16871	$17^h52^m17\overset{s}{.}68$	$-32°42'06\overset{''}{.}3$	13.82	14.84	0.028433525(10)	0.030864635(36)	–	–	–
16872	$17^h54^m35\overset{s}{.}55$	$-29°48'24\overset{''}{.}4$	15.21	16.17	0.033516366(13)	0.036939131(45)	0.04307991(13)	0.04435281(15)	0.04541343(15)
16873	$17^h58^m16\overset{s}{.}37$	$-27°54'43\overset{''}{.}8$	15.13	16.67	0.029935884(10)	0.034300425(12)	0.029934575(21)	0.039805145(49)	0.037234447(61)
16874	$17^h58^m30\overset{s}{.}84$	$-28°25'46\overset{''}{.}4$	13.86	14.62	0.0230617618(57)	0.0198797600(60)	0.053054509(54)	0.027531088(26)	0.024992040(24)
16875	$17^h58^m58\overset{s}{.}94$	$-28°03'42\overset{''}{.}6$	14.76	15.85	0.036425934(12)	0.042694792(45)	0.048473768(69)	0.09609703(28)	0.07844828(21)
16876	$17^h58^m59\overset{s}{.}19$	$-28°45'44\overset{''}{.}2$	14.61	15.48	0.030000956(11)	0.031942458(16)	–	–	–
16877	$18^h00^m49\overset{s}{.}06$	$-27°35'26\overset{''}{.}0$	13.82	14.59	0.0311231198(67)	0.041716525(14)	0.035578305(13)	0.033469123(20)	0.036362040(27)
16878	$18^h02^m25\overset{s}{.}70$	$-27°02'23\overset{''}{.}5$	14.48	15.41	0.0158377216(23)	0.0166989591(23)	0.0150967282(37)	0.0167467952(47)	0.0158803976(48)
16879	$18^h03^m25\overset{s}{.}04$	$-27°01'41\overset{''}{.}7$	14.78	15.61	0.0168271841(31)	0.0189019685(57)	0.017930385(11)	0.018901708(12)	0.019266537(18)
16880	$18^h05^m30\overset{s}{.}36$	$-28°28'49\overset{''}{.}4$	15.57	16.68	0.036513655(16)	0.042300103(34)	0.046980198(57)	0.036513303(41)	–
16881	$18^h15^m03\overset{s}{.}77$	$-27°33'06\overset{''}{.}7$	14.37	14.92	0.034369987(13)	0.022029517(14)	–	–	–
16882	$18^h16^m13\overset{s}{.}66$	$-26°53'15\overset{''}{.}3$	13.67	14.40	0.036765128(19)	0.048780768(51)	0.039913311(33)	0.047063512(55)	0.020849953(31)
16883	$18^h20^m37\overset{s}{.}13$	$-23°00'08\overset{''}{.}0$	14.62	15.64	0.034885725(23)	0.037769423(12)	0.0361497383(56)	–	–

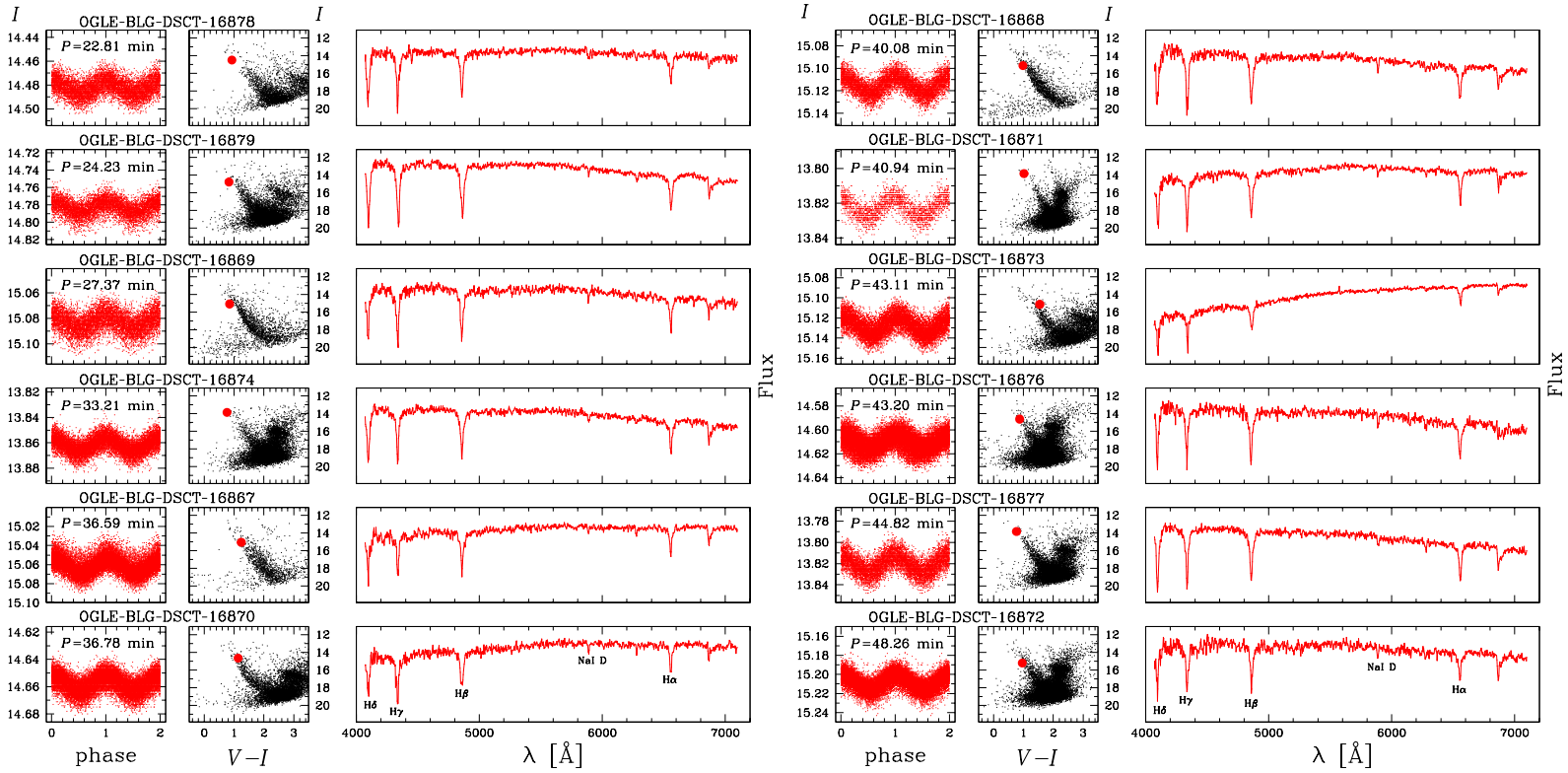

Fig. 1. Phased OGLE *I*-band light curves (*left column*), $V-I$ color *vs.* *I* magnitude diagrams (*middle column*), and EFOSC2 low-resolution spectra (*right column*) of 12 (out of 24) discovered δ Sct stars ordered with increasing pulsation period (provided in the *left column*).

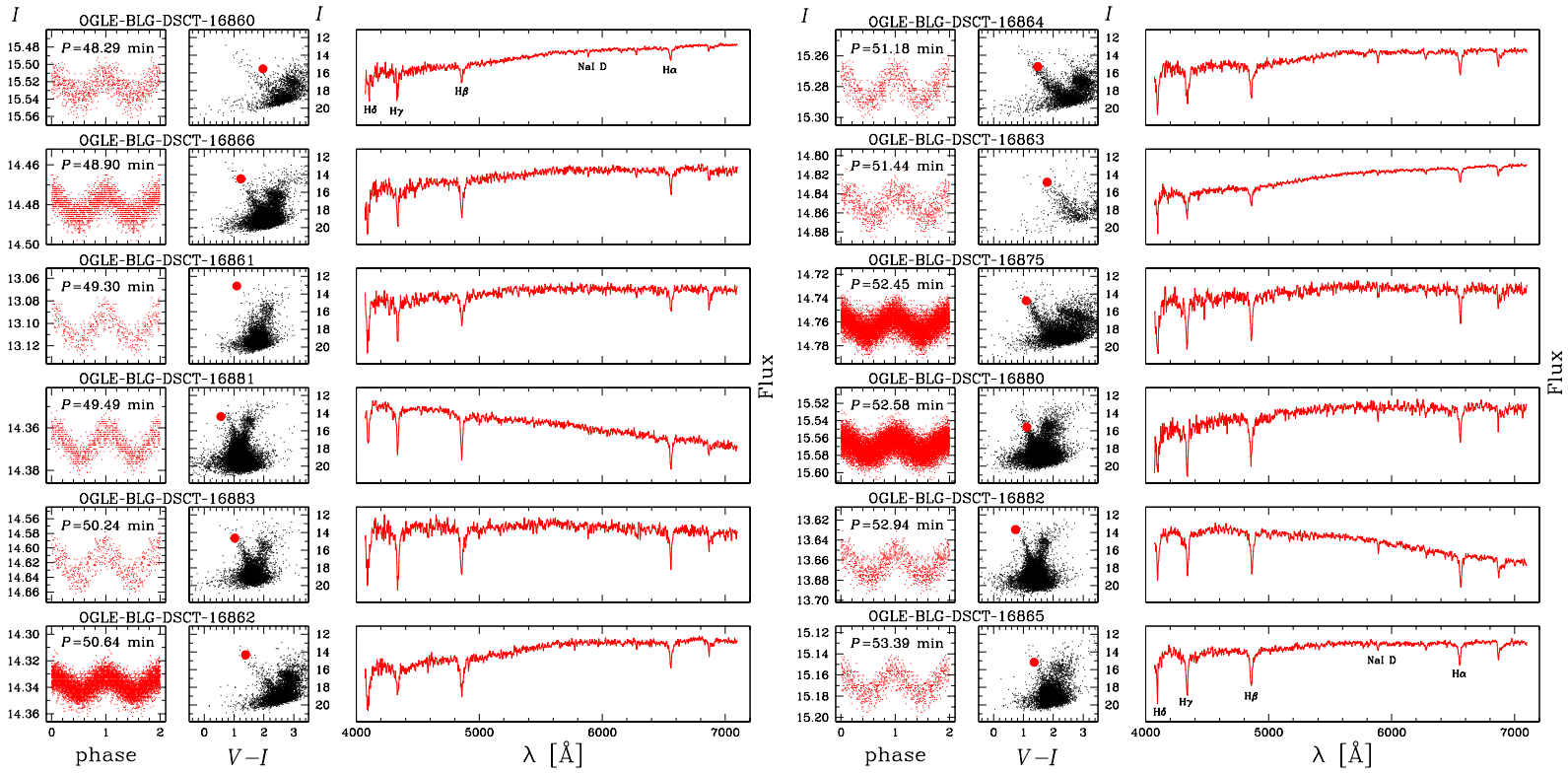

Fig. 2. Same as Fig. 1 for the remaining δ Sct stars.

T a b l e 2

Atmospheric parameters of the observed stars

Name OGLE-BLG-DSCT-	$T_{\rm eff}$ [K]	log$g$	Name OGLE-BLG-DSCT-	$T_{\rm eff}$ [K]	log$g$
16860	7950 ± 260	3.69 ± 1.23	16872	7450 ± 220	4.31 ± 0.92
16861	7610 ± 240	3.79 ± 1.03	16873	8170 ± 370	4.05 ± 1.05
16862	7840 ± 190	4.68 ± 1.12	16874	8090 ± 310	4.73 ± 1.07
16863	7570 ± 210	3.71 ± 0.64	16875	7770 ± 270	3.93 ± 0.83
16864	8010 ± 220	4.35 ± 0.85	16876	8710 ± 360	4.08 ± 0.61
16865	8230 ± 380	3.34 ± 0.58	16877	8130 ± 280	4.14 ± 0.91
16866	7650 ± 300	4.90 ± 0.82	16878	8750 ± 500	4.47 ± 0.65
16867	7730 ± 460	4.91 ± 0.80	16879	8930 ± 370	4.52 ± 0.39
16868	8095 ± 183	4.97 ± 0.88	16880	7870 ± 300	4.08 ± 0.69
16869	8410 ± 430	4.27 ± 1.06	16881	9480 ± 420	3.81 ± 0.62
16870	8160 ± 290	4.59 ± 0.91	16882	7370 ± 230	4.34 ± 0.96
16871	8390 ± 410	4.11 ± 0.83	16883	9180 ± 410	4.31 ± 0.68

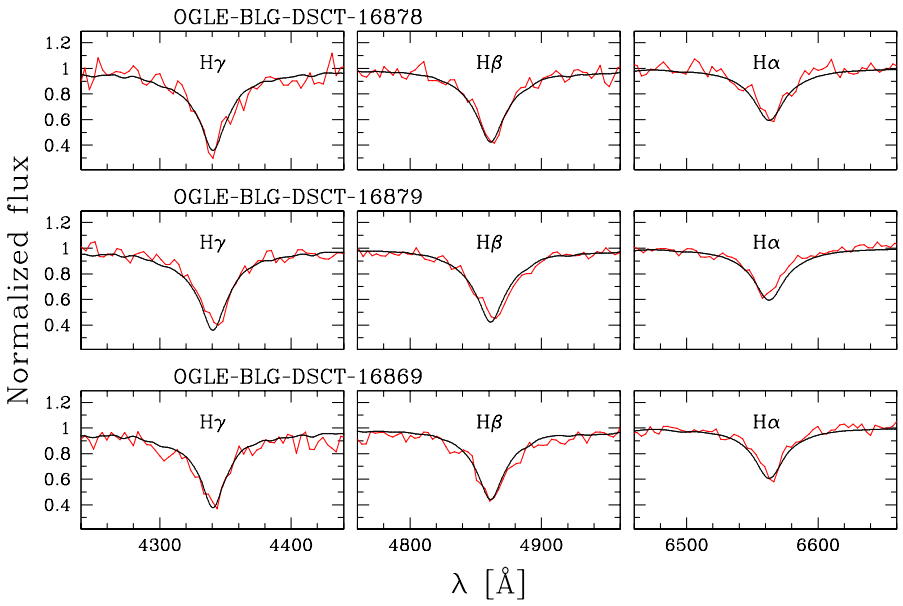

Fig. 3. Fits to hydrogen lines in three δ Sct stars with periods below 30 min.

Fig. 4 shows the location of the 24 stars in the $T_{\rm eff}$ *vs.* log$g$ plane. All the objects have the atmospheric parameters typical for the main sequence A/F stars. However, with the used spectral resolution, we cannot exclude that some objects slightly evolved off the MS. Nevertheless, the spectra confirm that all the stars are

located in the area populated by δ Sct-type variables in the Hertzsprung-Russell diagram.

We note that only one object, OGLE-BLG-DSCT-16883, was reported as a variable source in Gaia DR3 (Gaia Collaboration 2021), but it was incorrectly classified as a spotted star (of RS CVn type). Measured parallaxes of 23 stars are between 0.20 ± 0.06 mas and 0.82 ± 0.02 mas, which places them likely in the Galactic disk. The parallax of OGLE-BLG-DSCT-16864, 0.08 ± 0.06 mas, indicates a more distant location, probably the Galactic bulge.

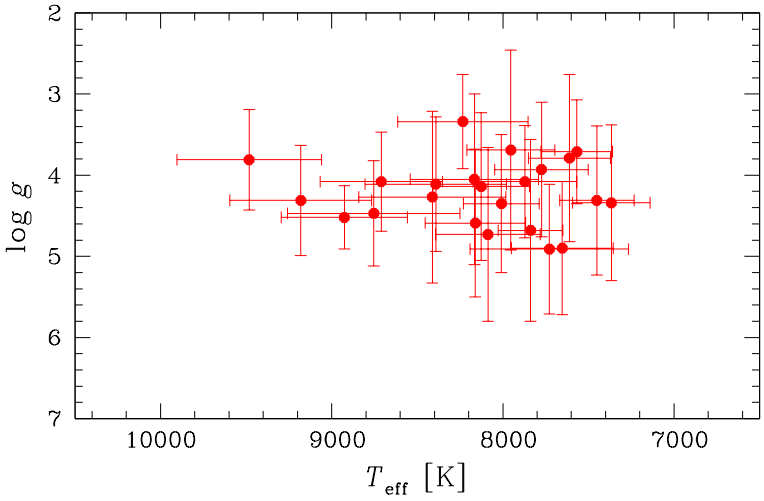

Fig. 4. Positions of the 24 observed stars in the $T_{\rm eff}$ *vs.* $\log g$ plane. All the objects are located in the area for MS stars of spectral type A and early F.

5. On-line Data

The newly confirmed δ Sct stars supplement the OCVS. The objects are arranged according to increasing right ascension and have names from OGLE-BLG-DSCT-16860 to OGLE-BLG-DSCT-16883. The photometric as well as spectroscopic data are available to the astronomical community through the OGLE On-line Data Archive at *https://ogle.astrouw.edu.pl*.

Acknowledgements. MG is supported by the EU Horizon 2020 research and innovation programme under grant agreement No 101004719. This work is based on observations collected at the European Southern Observatory under ESO programme 105.20EF.001. We used data from the European Space Agency (ESA) mission Gaia, processed by the Gaia Data Processing and Analysis Consortium (DPAC). Funding for the DPAC has been provided by national institutions, in particular the institutions participating in the Gaia Multilateral Agreement.

REFERENCES

Alard, C., and Lupton, R.H. 1998, *ApJ*, **503**, 325.
Asplund, M., Grevesse, N., Sauval, A.J., and Scott, P. 2009, *ARA&A*, **47**, 481.
Balona, L.A. 2022, *MNRAS*, **510**, 5743.
Balona, L.A., and Dziembowski, W.A. 2011, *MNRAS*, **417**, 591.
Blanco-Cuaresma, S., Soubiran, C., Heiter, U., and Jofré, P. 2014, *A&A*, **569A**, 111.
Blanco-Cuaresma, S. 2019, *MNRAS*, **486**, 2075.
Buzzoni, B., Delabre, B., Dekker, H., *et al.* 1984, *The Messenger*, **38**, 9.
Castelli, F., and Kurucz, R.L. 2003, *IAU Symp.*, **210**, A20, arXiv:astro-ph/0405087.
Gaia Collaboration, Brown, A.G.A., *et al.* 2021, *A&A*, **649**, A1.
Heber, U. 2016, *PASP*, **128**, 966.
Holdsworth, D.L., Smalley, B., Gillon, M., *et al.* 2014, *MNRAS*, **439**, 2078.
Iwanek, P., Soszyński, I., Skowron, J., *et al.* 2019, *ApJ*, **879**, 114.
Kaluzny, J., Olech, A., Thompson, I.B., *et al.* 2004, *A&A*, **424**, 1101.
Kupfer, T., Bauer, E.B., Burdge, K.B., *et al.* 2019, *ApJ*, **878**, L35.
Kurtz, D.W. 2022, *ARA&A*, **60**, 31.
Kurucz, R.L. 2005, *Memorie della Società Astronomica Italiana Supplement*, **8**, 14.
Maxted, P.F.L., Serenelli, A.M., Miglio, A., *et al.* 2013, *Nature*, **498**, 463.
Mróz, P., Udalski, A., Poleski, R., *et al.* 2015, *Acta Astron.*, **65**, 313.
Murphy, S.J., Hey, D., Van Reeth, T., and Bedding, T.R. 2019, *MNRAS*, **485**, 2380.
Netzel, H., Pietrukowicz, P., Soszyński, I., and Wrona, M. 2022, *MNRAS*, **510**, 1748.
Pawlak, M., Soszyński, I., Udalski, A., *et al.* 2016, *Acta Astron.*, **66**, 421.
Pietrukowicz, P., Dziembowski, W.A., Latour, M., *et al.* 2017, *Nature Astronomy*, **1E**, 166.
Pietrukowicz, P., Soszyński, I., Netzel, H., *et al.* 2020, *Acta Astron.*, **70**, 241.
Piskunov, N.E., Kupka, F., Ryabchikova, T.A., Weiss, W.W., and Jeffery, C.S. 1995, *A&AS*, **112**, 525.
Quirion, P.-O., Fontaine, G., and Brassard, P. 2007, *ApJS*, **171**, 219.
Rodríguez, E., López-González, M.J., and López de Coca, P. 2000, *A&AS*, **144**, 469.
Rodríguez, E., and López-González, M.J. 2000, *A&A*, **359**, 597.
Schwarzenberg-Czerny, A. 1996, *ApJ*, **460**, L107.
Soszyński, I., Poleski, R., Udalski, A., *et al.* 2008, *Acta Astron.*, **58**, 163.
Soszyński, I., Udalski, A., Wrona, M., *et al.* 2019, *Acta Astron.*, **69**, 321.
Soszyński, I., Pietrukowicz, P., Skowron, J., *et al.* 2021, *Acta Astron.*, **71**, 189.
Udalski, A., Szymański, M.K., and Szymański, G. 2015, *Acta Astron.*, **65**, 1.
Winget, D.E., and Kepler, S.O. 2008, *ARA&A*, **46**, 157.
Woźniak, P.R. 2000, *Acta Astron.*, **50**, 421.
Wrona, M., Ratajczak, M., Kołaczek-Szymański, P.A., *et al.* 2022, *ApJS*, **259**, 16.